Nanoscale

PAPER

View Article Online
View Journal

Cite this: DOI: 10.1039/d6nr00514d

Atomic-level design principles for the hydrogen evolution reaction on high-entropy MXene catalysts

Hao Yuan, Jing Yang and Yong-Wei Zhang*

High-entropy materials, with their rich compositional diversity, offer an exceptional platform for tailoring catalytic performance through synergistic interactions among multiple metal elements. This inherent heterogeneity gives rise to a wide distribution of local atomic environments, resulting in a broad spectrum of binding energies for catalytic intermediates. In this work, we investigate the hydrogen evolution reaction (HER) on high-entropy MXenes (HE-MXenes) by combining high-throughput density functional theory (DFT) calculations with machine learning, aiming to uncover atomic-scale design principles that govern catalytic activity. Specifically, we systematically probe hydrogen adsorption across a statistically diverse set of local environments on $TiVNbMoC_3O_2$ surfaces. While Mo-based MXenes are widely regarded as highly active HER catalysts in pristine or low-component systems, our results demonstrate that, in HE-MXenes, catalytic behavior is governed primarily by the local atomic coordination rather than by the identity of any single metal species. In particular, our findings reveal that the identity of the first-nearest neighbor shell to the surface oxygen termination plays a dominant role in determining HER activity, with the activity following the trend V < Mo < Ti < Nb within the first shell. Notably, configurations such as Nb_3, Ti_1Nb_2 and Nb_2Mo_1 exhibit particularly outstanding performance. To elucidate the underlying factors, we employ machine learning and identify the average covalent radius of neighboring metal atoms as a key descriptor governing adsorption behavior. This insight enables rapid, descriptor-based screening of high-performance HER catalysts without the need for exhaustive DFT calculations. Overall, our work highlights the pivotal role of local atomic environments in catalytic activity and establishes an efficient, data-driven platform to accelerate the discovery of HE-MXenes for next-generation electrocatalysis.

Received 6th February 2026,
Accepted 17th May 2026

DOI: 10.1039/d6nr00514d

rsc.li/nanoscale

Introduction

As global efforts intensify to mitigate climate change, the urgent need for sustainable and renewable energy sources has never been more critical. Hydrogen energy, with its high energy density and zero-carbon emissions upon combustion, is emerging as a cornerstone in the transition toward a low-carbon economy.[1] Unlike conventional fossil fuels, hydrogen generates only water as a byproduct, making it an ideal energy carrier for reducing greenhouse gas emissions across multiple sectors, including transportation, power generation, and heavy industry.[2,3] As nations and industries set ambitious carbon-neutrality targets, hydrogen is increasingly recognized as a pivotal enabler of global energy transformation. However, unlocking its full potential as a clean energy vector requires the development of cost-effective, scalable, and environmentally sustainable hydrogen production technologies.[4]

Among various hydrogen production methods, three dominant approaches exist: (1) thermochemical processes such as steam methane reforming, which currently dominate industrial hydrogen production but suffer from high CO_2 emissions;[5,6] (2) biomass-derived hydrogen, which offers a renewable alternative but is limited by scalability challenges;[7,8] and (3) electrochemical water splitting, which presents a promising route to green hydrogen when powered by renewable electricity.[9,10] In this context, the hydrogen evolution reaction (HER), which occurs at the cathode during water electrolysis, plays a pivotal role in determining overall energy efficiency. A major bottleneck in HER technology is the lack of affordable and efficient catalysts that can facilitate hydrogen evolution with low overpotentials and high durability.[11] Platinum (Pt) and other precious metal-based catalysts remain the benchmark for the HER due to their exceptional catalytic activity and stability.[10,12] However, their high cost, limited availability, and susceptibility to deactivation under harsh operating conditions

*Institute of High Performance Computing (IHPC), Agency for Science, Technology and Research (A*STAR), 1 Fusionopolis Way, #16-16 Connexis, Singapore 138632, Republic of Singapore*

significantly hinder their large-scale deployment. Therefore, developing alternative catalysts that can achieve comparable or superior HER performance while being cost-effective and earth-abundant is a pressing research priority.

MXenes, a unique class of two-dimensional (2D) transition metal carbides and nitrides, have garnered significant attention as promising electrocatalysts for the HER.[13,14] Comprising transition metal layers interleaved with carbon or nitrogen and terminated with functional groups such as oxygen, fluorine, or hydroxyl, MXenes exhibit remarkable chemical versatility. Their electronic properties can be precisely tuned through element substitution and surface modification, making them attractive candidates for electrocatalytic applications.[15] The catalytic potential of MXenes has been extensively studied. Seh *et al.* first demonstrated the HER activity of Mo_2CT_x, highlighting their intrinsic electrocatalytic capabilities.[13] Bai *et al.* further expanded this understanding through a high-throughput computational screening of 20 MXenes, identifying Ti_2NO_2 and Nb_2NO_2 as HER-active materials with performance approaching that of Pt.[16] Moreover, recent investigations into double-transition-metal MXenes have unveiled a new avenue for HER optimization, where the combination of different transition metals allows tunability in adsorption strength and catalytic activity.[17–19] Notably, $Mo_2NbC_2O_2$ has emerged as a promising HER catalyst due to its low overpotential and balanced adsorption characteristics.

Building upon these advances, the recent synthesis of high-entropy MXenes (HE-MXenes) such as $TiVNbMoC_3$ and $TiVCrMoC_3$ has opened new frontiers in catalyst design.[20] HE-MXenes, characterized by their multielement composition, introduce an unprecedented level of tunability in catalytic properties by leveraging the synergistic effects of multiple transition metals. This high configurational entropy not only stabilizes the MXene structure but also provides vast compositional flexibility for optimizing HER performance. By precisely controlling the local electronic environment and adsorption characteristics, HE-MXenes represent a new generation of customizable, efficient, and cost-effective catalysts.

However, the rational design of HE-MXenes for hydrogen evolution remains in its infancy, with several fundamental challenges that must be addressed to fully exploit their catalytic potential. The inherent structural and compositional complexity of HE-MXenes raises critical questions about how local atomic configurations govern catalytic activity. Specifically, how does the identity and distribution of neighboring metal atoms influence hydrogen adsorption energetics and active site formation? In addition, the vast compositional design space necessitates efficient screening strategies, raising the question of whether robust descriptors can be identified to predict catalytic performance without exhaustive computation. Addressing these questions is essential for establishing predictive design principles and unlocking the full potential of HE-MXenes as a new class of HER catalysts.

In this work, we conduct high-throughput density functional theory (DFT) simulations to systematically explore the HER activity of HE-MXenes by generating random configurations that capture diverse local atomic environments. Our results reveal that the identity of the first-nearest neighbor to the active oxygen site is the dominant factor governing hydrogen adsorption behavior, while contributions from more distant neighbors act as minor perturbations. A clear activity trend is observed among neighbouring elements, following the order V < Mo < Ti < Nb, with Nb- and Ti-rich environments showing the most favourable HER performance. Leveraging machine learning, we identify the average covalent radius of first-neighbor metal atoms as a decisive descriptor for predicting hydrogen adsorption free energy. This intrinsic property enables efficient, descriptor-driven screening of HER activity, significantly reducing computational costs. Given the correlation between intrinsic properties and catalytic performance, these findings provide important insights into the role of the local atomic environment in governing hydrogen adsorption behavior in $TiVNbMoC_3O_2$ and suggest that such descriptors may serve as useful guidelines for the rational design of high-entropy MXene catalysts, although further validation across different compositions is required.

Computational details

All simulations were conducted using the Vienna *ab initio* simulation package (VASP) within a DFT framework, utilizing the projector augmented-wave (PAW) method.[21,22] The exchange–correlation functional employed was the Perdew–Burke–Ernzerhof (PBE) formulation within the generalized gradient approximation (GGA).[23–25] An energy cutoff of 500 eV was applied with convergence thresholds set at 10^{-5} eV for energy and −0.02 eV Å^{-1} for force. van der Waals interactions were accounted for using the DFT-D3 correction.[26] To prevent interactions between periodic images, a 15 Å vacuum layer was introduced. Here, the HER in an acidic environment is considered, represented by the reaction

$$2H^+ + 2e^- \rightarrow H_2.$$

The Gibbs free energy for hydrogen adsorption, ΔG_H, is determined using the computational hydrogen electrode (CHE) model as[27]

$$\Delta G_H = \Delta E_H + \Delta ZPE - T\Delta S_H,$$

where ΔE_H, ΔZPE, and ΔS_H correspond to the differences in electronic energy, zero-point energy, and entropy, respectively.

A microkinetic model was employed to estimate current densities. For cases where $\Delta G_H > 0$, the current density is calculated as follows:[28]

$$i_0 = \frac{-eck_0 e^{-\Delta G_H/k_B T}}{1 + e^{-\Delta G_H/k_B T}}.$$

For cases where $\Delta G_H < 0$, the current density is given by

$$i_0 = \frac{-eck_0}{1 + e^{-\Delta G_H/k_B T}},$$

where e, k_0, k_B and T represent the elementary charge, rate constant, Boltzmann constant, and temperature, respectively. In

this work, k_0 is treated as a constant prefactor and is set to 2×10^{17} s^{-1} cm^{-2}, while $T = 300$ K.

In this study, we investigated the experimentally synthesized high-entropy MXene $TiVNbMoC_3$ 20 with oxygen termination. It was shown that oxygen termination was able to provide optimal adsorption energetics, higher catalytic activity, and greater structural/electrochemical stability than fluorine and hydroxyl terminations.[29] This makes O-terminated HE-MXenes a superior platform for rational HER catalyst design using atomic-level descriptors and high-throughput screening. To model the structural complexity of high-entropy MXenes, we generated randomized configurations using a $4 \times 4 \times 1$ supercell of $Ti_4C_3O_2$. In each configuration, Ti atoms were randomly substituted by Ti, V, Nb, and Mo while maintaining an overall equimolar composition (1 : 1 : 1 : 1). The substitution was performed without imposing any artificial ordering constraints, allowing for a diverse sampling of local atomic environments. Multiple independent configurations were generated to capture different local coordination motifs. The lattice constant was estimated as the weighted average of the lattice parameters of $Ti_4C_3O_2$, $V_4C_3O_2$, $Nb_4C_3O_2$, and $Mo_4C_3O_2$, providing a representative structural framework for subsequent calculations.

To assess whether lattice distortion affects hydrogen adsorption energies, we compared calculations using both a fixed and a fully relaxed lattice in a random configuration. The results, summarized in Fig. S1, show that the difference in the adsorption energy of hydrogen adsorption is minimal at all active sites, indicating that the lattice relaxation has a relatively minor effect on the adsorption strength compared to local chemical environments. Given the high configurational entropy of $TiVNbMoC_3O_2$ MXene, a diverse range of local atomic environments is possible. In this study, we primarily focused on the influence of the first (S1) to fourth nearest (S4) neighbors surrounding the active oxygen site, while neglecting interactions beyond S4 due to electrostatic screening effects, as illustrated in Fig. 1. We also note that the studied structures are based on experimentally reported compositions, and the high configurational entropy is expected to contribute to the stabilization of the disordered phase. A detailed evaluation of surface thermodynamic stability (*e.g.*, surface energy or segregation effects) is beyond the scope of this work and will be addressed in future studies.

To systematically capture the variation in local chemical environments, we generated 32 unique HE-MXene configurations, which include 1024 data points, and computed the Gibbs free energy of hydrogen adsorption at each surface oxygen site. This dataset provides a foundation for understanding the role of the local atomic environment in tuning HER activity and serves as an input for further machine-learning analysis to establish structure–property relationships in HE-MXenes.

Results and discussion

The distribution of hydrogen adsorption free energies is shown in Fig. 2a. The different local environments around the adsorption site leads to a wide range of adsorption free energy

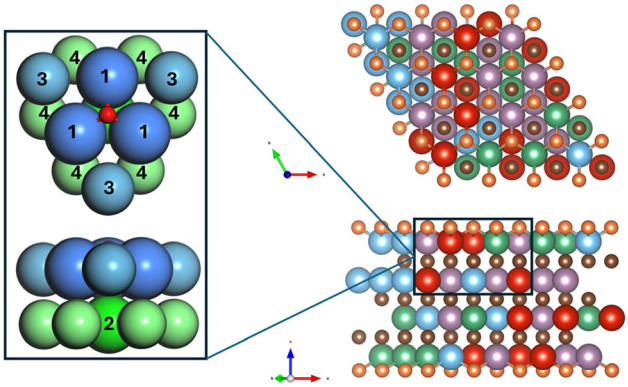

Fig. 1 Schematic diagram illustrating the high-entropy configurations based on nearest neighbors. In the zoomed-in view on the left, dark blue indicates the first-nearest neighbors. Dark green, located directly beneath the active O site, represents the second-nearest neighbor. Light blue, in the same layer as the first-nearest neighbors, denotes the third-nearest neighbors. The fourth-nearest neighbors, shown in light green, are positioned in the same layer as the second-nearest neighbors.

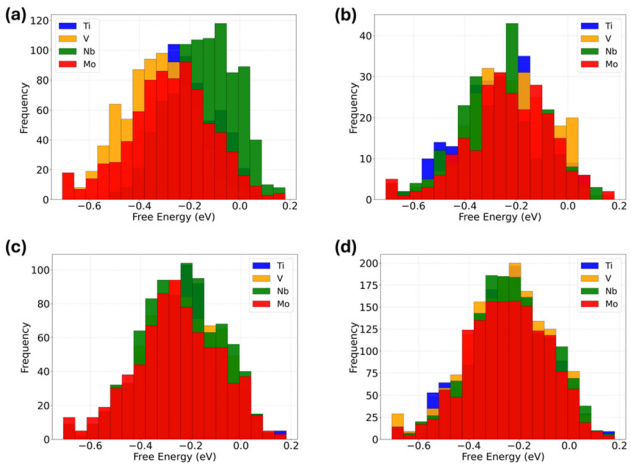

Fig. 2 (a) Distribution of total free energies for various HE-MXene configurations, highlighting the thermodynamic diversity arising from local atomic environments. (b) Correlation between the HER exchange current density and the Gibbs free energy of hydrogen adsorption, illustrating the volcano-type relationship and identifying optimal catalytic performance near $\Delta G_H \approx 0$ eV.

from −0.7 eV to 0.15 eV, which verified the advantages of HE-MXenes with tunable adsorption. The theoretical relationship between the exchange current density (i_0) and ΔG_H is illustrated in Fig. 2b. The volcano-shaped trend highlights the optimal catalytic activity near $\Delta G_H \approx 0$ eV. Notably, a substantial fraction of HE-MXenes exhibit ΔG_H values closer to the thermoneutral point than those of conventional MXenes and Pt (see Table S1), highlighting their potential for superior HER catalytic performance.

A closer examination of the elemental distribution from the first to fourth neighbor shells (see Fig. 3) reveals distinct trends, particularly in the first-neighbor environment. The dis-

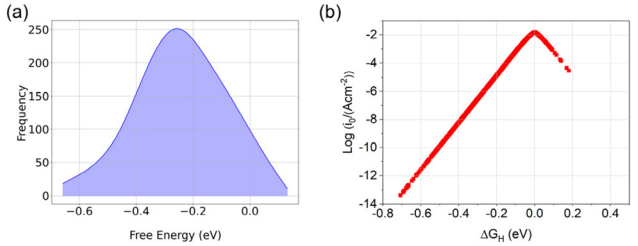

Fig. 3 Adsorption free energy distribution for (a) first, (b) second, (c) third, and (d) fourth nearest neighbors. Each curve represents the frequency of metals at the corresponding energy. Ti, V, Nb, and Mo are plotted in red, green, blue, and purple, respectively. The filled color gradient from yellow to pink represents the frequency from high to low.

tribution profiles show clear differences in the peak positions and elemental frequencies, indicating a pronounced effect of the first-neighbor composition on the hydrogen adsorption free energy. Notably, the center of the free energy shifts with the trend V (−0.353 eV) < Mo (−0.294 eV) < Ti (−0.264 eV) < Nb (−0.163 eV), suggesting that V-rich first-neighbor environments tend to exhibit stronger H adsorption, whereas Nb-rich environments correspond to weaker adsorption. This finding implies that the first-neighbor shell plays a dominant role in modulating the local adsorption strength, likely due to direct electronic and geometric interactions with the adsorption site.

In contrast, the elemental distributions for the second, third, and fourth neighbors show considerably less variation across different elements, with largely overlapping frequency curves and similar distribution widths and centers. This indicates that the influence of these more distant neighbors on adsorption free energy is relatively minor, possibly due to their diminished electronic coupling and spatial separation from the adsorption site. The results emphasize the critical role of the immediate local chemical environment (first-neighbor shell) in determining HER activity and highlight the importance of engineering the local atomic configuration around active sites in high-entropy MXenes for optimal catalytic performance. The effect of shell distance is further analyzed as shown in Fig. 4. The figure presents the distribution of neighboring elemental distances within specific free energy windows, further clarifying the relationship between local atomic configuration and hydrogen adsorption strength. Notably, the S2 and S3 neighbors exhibit nearly identical distance distributions relative to the active oxygen site. Furthermore, no distinct distribution preferences are observed

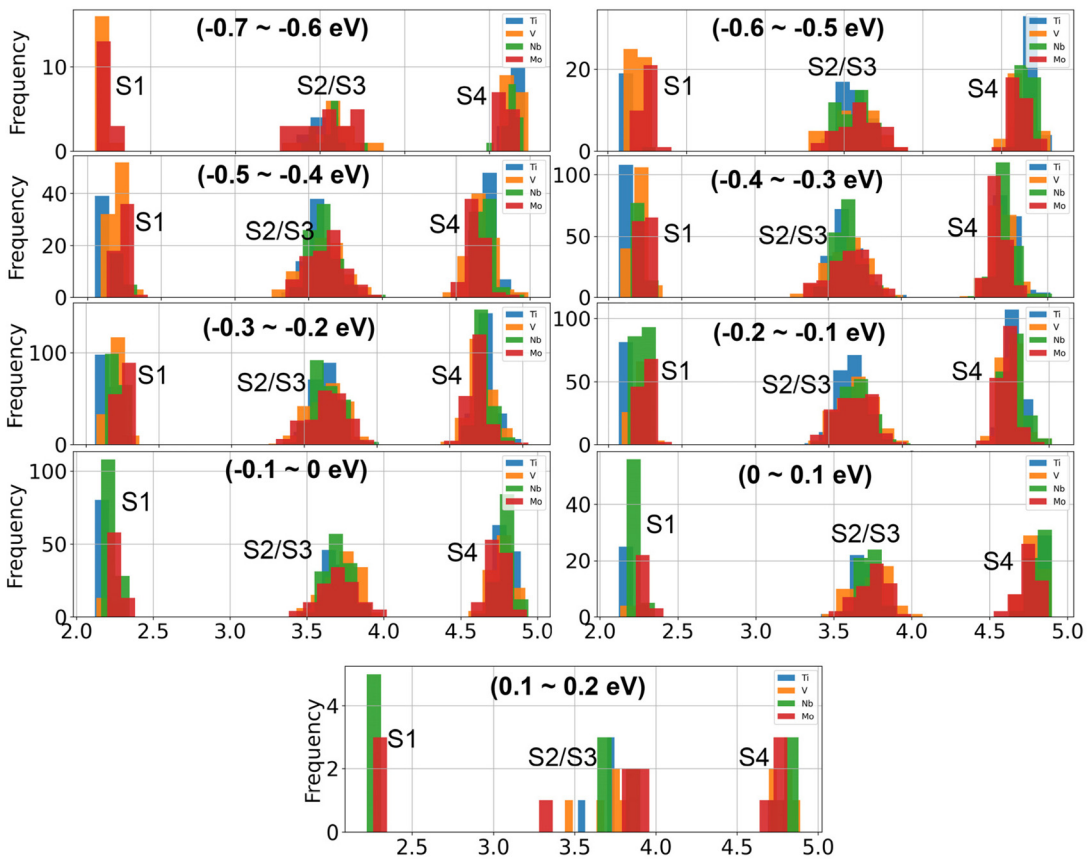

Fig. 4 Frequency distribution of metal–oxygen bond lengths for four elements (Ti, V, Nb, and Mo) across different adsorption free energy ranges from −0.7 eV to 0.2 eV. In each plot, the first to fourth neighbors are shown from left to right. Ti, V, Nb, and Mo are represented by blue, yellow, green, and red, respectively.

across different energy windows. V and Mo show broader distance distributions, whereas Nb and Ti display narrower, more localized distributions. A similar trend is also observed for the S4 neighbors. These results support the earlier conclusion that S2 to S4 neighbors contribute marginally to the overall adsorption free energy variation. However, for S1, a clear dependence on free energy becomes evident. In the most negative adsorption free energy regions (−0.7 to −0.6 eV), the distribution is dominated by V and Mo atoms, indicating that these elements in the first-neighbor shell are likely responsible for strong hydrogen binding. This trend reinforces the idea that V and Mo enhance the electronic environment conducive to strong adsorption interactions. In contrast, in the moderate free energy range (*e.g.*, −0.1–0 eV and 0–0.1 eV), Nb becomes increasingly dominant, followed by Ti, suggesting that Nb-rich and Ti-rich first-neighbor environments contribute to the appropriate magnitude of H binding, aligning with the previous analysis in Fig. 3. Since the optimal free energy range is −0.1–0.1 eV, Nb and Ti are ideal neighboring elements for high-performance HER. Overall, these findings underscore the critical role of first-shell composition and distance while also validating the negligible impact of outer shells (S2–S4). Such insights are invaluable for rational catalyst design, where local structural motifs can be tailored to optimize hydrogen binding energy and hence HER performance.

To further understand the S1 distribution–activity relationship, the distributions of ΔG_H for all possible combinations of Ti, V, Nb, and Mo in the first-neighbor shell are shown in Fig. 5. A total of 19 elemental configurations, including pure (M_3) and mixed ($M_1M_2M_3$) compositions, are analyzed to capture the statistical range of hydrogen adsorption free energies. A clear activity trend can be observed among the pure configurations, where Nb_3 shows the weakest adsorption, followed by Ti_3, while Mo_3 and V_3 exhibit stronger adsorption,

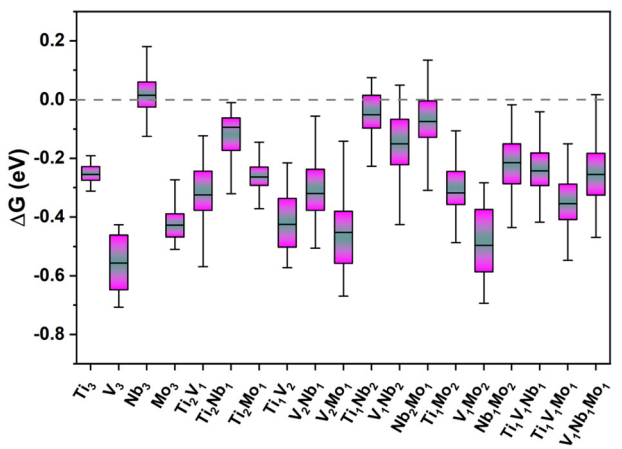

Fig. 5 Box plots of Gibbs free energy of hydrogen adsorption for various first-neighbor environments in high-entropy MXenes. Each box represents the interquartile range (IQR) with the median marked by a horizontal line, while the whiskers denote the range of the data excluding outliers. The optimal position of $\Delta G_H \approx 0$ eV is shown by the grey dashed line.

establishing the trend: $V_3 > Mo_3 > Ti_3 > Nb_3$. This finding aligns well with earlier analysis, highlighting the role of specific elements in tuning adsorption strength. Among these, Nb_3- and Nb-dominated combinations, such as Ti_1Nb_2 and Nb_2Mo_1, exhibit the most favorable distributions, with peaks centered near 0 eV. The relatively small interquartile ranges, especially for Ti_1Nb_2, in these mixed combinations also indicate robust performance stability across different local atomic arrangements. This further strengthens the conclusion that local chemical composition in the S1 shell plays a decisive role in tuning HER activity, and strategic elemental mixing is a promising pathway toward high-efficiency high-entropy MXene catalysts.

To further evaluate the effect of lattice strain (*i.e.*, shrinkage or expansion), we computed ΔG_H for pure MXenes constrained to the lattice constant of the HE-MXenes ($a = b = 3.04$ Å). Notably, the lattice constants of $Ti_4C_3O_2$ (3.04 Å) and $Mo_4C_3O_2$ (3.05 Å) are well aligned with that of the HE-MXene, indicating that the ΔG_H variations in Ti_3- and Mo_3-dominated local environments are primarily governed by the chemical environment rather than by strain. In the case of $V_4C_3O_2$, which undergoes a modest expansion (from 2.92 Å to 3.04 Å), ΔG_H remains nearly unchanged (−0.46 *vs.* −0.49 eV), further supporting the dominance of local environment-driven variations. Conversely, $Nb_4C_3O_2$ experiences notable compression under the HE-MXene lattice (from 3.15 Å to 3.04 Å), resulting in a moderate ΔG_H increase of 0.18 eV. This indicates that while Nb is somewhat more responsive to lattice distortion, the overall impact of lattice strain on adsorption strength remains limited compared to the influence of the local chemical environment. Overall, these findings underscore the critical importance of precisely tuning the elemental composition and local atomic environment in HE-MXenes to optimize HER activity.

To gain deeper insight into the relationship between local atomic environments and hydrogen adsorption behavior in HE-MXenes, we deployed machine learning models to predict the hydrogen adsorption free energy.[30] The dataset consists of adsorption energies obtained from density functional theory calculations for 1024 adsorption sites, each described by a set of seven descriptors capturing atomic, geometric, and electronic features. The dataset was randomly divided into training (75%) and test (25%) sets. Three ensemble learning models were employed: Random Forest Regressor (RFR), Gradient Boosting Regressor (GBR), and Extra Trees Regressor (ETR), which are well-suited for modeling non-linear relationships in complex systems. Hyperparameters for each model were optimized using cross-validation. Model performance was evaluated using the coefficient of determination (R^2) and root mean squared error (RMSE). The use of multiple models allows us to assess the robustness of the identified structure–property relationships and ensure that the conclusions are not dependent on a specific algorithm. These models employ a diverse set of descriptors, including intrinsic properties (average covalent radius (ACR), average electronegativity (AEN), and average ionization energy (AIE)), as well as post-adsorption fea-

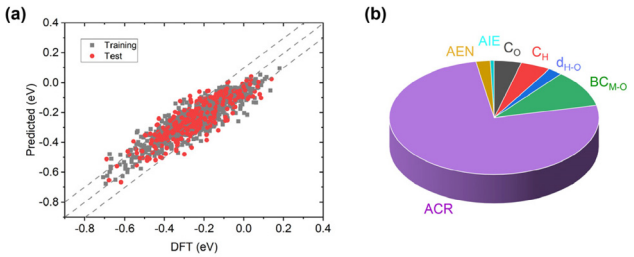

Fig. 6 (a) Scatter plot comparing machine learning-predicted hydrogen adsorption free energies with DFT-calculated values for both the training set (gray squares) and the test set (red circles). The dashed lines represent ±0.1 eV deviations from perfect agreement. (b) Feature importance analysis presented as a pie chart, showing the relative contributions of different descriptors to the ML model.

tures derived from DFT calculations, such as electronic properties (charge on O (C_O) and charge on H (C_H)) and bond-related characteristics (H–O bond length (d_{H-O}) and changes in metal–O bond length (BC_{M-O})). All models exhibit strong predictive performance as shown in Fig. S2. Among them, the GBR model outperforms the others, achieving an R^2 score of 0.8 on the training set and 0.74 on the test set. The root mean square errors (RMSE) for both sets are below 0.1 eV, indicating high accuracy. Detailed model performance is illustrated in Fig. 6a, where predicted ΔG_H values are plotted against DFT-calculated values for both training (grey squares) and test (red circles) datasets. The GBR model demonstrates excellent predictive capability, as most data points lie close to the ideal diagonal line, indicating strong agreement with DFT results. The narrow distribution within ±0.1 eV for both training and test datasets confirms the robustness and generalizability of the model without signs of overfitting.

To further understand the relationship between target ΔG_H and selected descriptors, the feature importance distribution is extracted, as shown in Fig. 6b. Notably, the intrinsic property of ACR exhibits the highest contribution at 76%, emphasizing its dominant role in modulating hydrogen adsorption free energy. The contributions from other descriptors, such as metal–O bond length change, are comparatively smaller but still provide supplementary influence. These results validate the use of ACR as a reliable and physically meaningful descriptor for fast screening of HER activity in HE-MXenes.

Discussion

The successful synthesis of HE-MXenes such as $TiVNbMoC_3$ and $TiVCrMoC_3$ by Nemani *et al.*[20] established the feasibility of entropy-stabilized 2D carbides and demonstrated their structural robustness and metallic conductivity. These findings motivated theoretical exploration of how compositional disorder can tune catalytic properties. More broadly, recent advances in high-entropy materials for the HER have highlighted that compositional complexity and diverse local coordination environments can significantly enhance catalytic activity and stability, offering new opportunities beyond conventional catalysts.[31,32] Earlier computational studies, however, largely examined ordered or double-transition-metal MXenes. For instance, Jin *et al.*[18] and Zeng *et al.*[33] identified promising ordered $M'_2M'C_2O_2$ combinations by varying metal identity and termination, revealing trends in ΔG_H but overlooking the broad distribution of local atomic environments intrinsic to HE-MXenes. Seong *et al.*[34] further analyzed synthesizability criteria but did not address catalytic behavior. In addition, recent mechanistic studies have begun to explore structure–property relationships in high-entropy catalysts, emphasizing the role of local coordination and electronic structure modulation in governing HER activity.[35] Consequently, a quantitative understanding of how configurational disorder governs HER activity has remained lacking.

Our study fills this gap by statistically mapping hydrogen adsorption across more than 1000 adsorption sites in the $TiVNbMoC_3O_2$ MXene. By explicitly sampling random local configurations, we reveal that the S1 shell exerts a dominant influence on ΔG_H, following the adsorption trend V > Mo > Ti > Nb, while contributions from S2–S4 neighbors are negligible (Fig. 3 and 4). This first-shell dominance provides a microscopic rationale for the enhanced HER activity observed in multielement or HE-MXenes. Our results attribute the near-thermoneutral adsorption to the presence of Nb- and Ti-rich local motifs. Although direct HER measurements on $TiVNbMoC_3O_2$ itself remain limited, our findings offer a mechanistic foundation explaining the favorable trends observed in this family of HE-MXenes. We note that the widely reported superiority of Mo-based MXenes is largely derived from studies on pristine or low-component systems.[13] In contrast, the present work focuses on high-entropy MXenes, where HER activity is governed primarily by the local atomic environments rather than by the identity of a single metal species. Our results indicate that Nb-rich local configurations (*e.g.*, $TiNb_2$, Nb_2Mo, and Nb_3) provide a more optimal balance of hydrogen adsorption strength, whereas Mo-rich sites tend to overbind H, leading to more negative and thus less favorable ΔG_H. Importantly, this finding does not contradict established trends for Mo-based MXenes; rather, it highlights the breakdown of conventional single-element descriptors when applied to chemically complex, high-entropy MXene catalysts.

In comparison with earlier descriptor-based approaches, which typically relied on d-band centers or electronegativity differences, we identify the average covalent radius (ACR) of first-neighbor metals as a single, physically meaningful descriptor capturing the variance in ΔG_H. The ACR descriptor unifies geometric and electronic effects—smaller radii enhance orbital overlap and strengthen O–H bonding, whereas larger radii weaken adsorption—thus providing an intuitive design rule that complements the more empirical ML fingerprints used for HEAs and carbides. This interpretable, low-dimensional descriptor enables rapid, DFT-free screening of HE-MXene compositions and aligns with recent ML advances in high-entropy alloy catalysis, where local geometric metrics outperform complex electronic ones.[36–38]

To understand the physical origin of the average covalent radius (ACR) descriptor, we emphasize that ACR is defined based on the local coordination environment surrounding the active O site, considering only the neighboring metal atoms. This local definition is particularly important for high-entropy MXenes, where significant compositional disorder leads to highly heterogeneous active sites. Unlike conventional descriptors such as the d-band center, which are typically defined for uniform surfaces, it is challenging to uniquely assign a local d-band center to a specific adsorption site in such disordered systems. In contrast, ACR provides a well-defined and intuitive measure of the local atomic environment. Physically, ACR reflects the average atomic size of neighboring metals and thus governs local lattice distortion and strain. Variations in ACR lead to changes in metal–oxygen bond lengths and coordination geometry, which in turn affect the hybridization between metal d orbitals and oxygen p orbitals. These changes modulate the local electronic structure and charge distribution, ultimately influencing the hydrogen adsorption free energy (ΔG_H).

Therefore, ACR can be regarded as an effective local structural descriptor that captures the essential geometric features of the active site and their impact on adsorption behavior in high-entropy MXenes.

For different machine learning models, multiple machine learning models were employed to ensure the robustness and reliability of the identified descriptors. Specifically, we used different regression approaches to verify that the observed relationships between descriptors and ΔG_H are not dependent on a specific model choice. The consistent identification of key descriptors across different models increases confidence in their physical relevance. Regarding model performance, an R^2 value of 0.74 on the test set is considered reasonable given the intrinsic complexity of high-entropy MXenes. In such systems, hydrogen adsorption is influenced by highly heterogeneous local environments, leading to significant variability that is challenging to fully capture with a limited set of descriptors. Moreover, the primary goal of this work is not to achieve maximum predictive accuracy but to identify physically interpretable descriptors that reveal the underlying structure–property relationships. Therefore, the obtained accuracy represents a good balance between predictive capability and interpretability and is sufficient to support the conclusions drawn in this study.

Beyond explaining existing results, this work establishes a general framework for the rational design of disordered 2D catalysts. First, site statistics are crucial—HE-MXene activity should be viewed as a distribution of ΔG_H rather than a single averaged value. Second, local composition control offers a practical lever: targeted surface enrichment of Nb/Ti near terminations or mild annealing that biases first-shell statistics could increase the fraction of optimal sites.[39] Third, descriptor transferability is key: because ACR is an intrinsic atomic property, it can be readily extended to other HE-MXenes (*e.g.*, $TiVCrMoC_3$) and to related reactions such as the OER and CO_2RR.

In the broader context of high-entropy materials and HEAs, our DFT + ML pipeline provides a site-resolved, data-driven design paradigm that bridges atomic-scale understanding with macroscopic catalytic performance. Future studies combining explicit solvation, coverage-dependent kinetics, and operando spectroscopic validation (*e.g.*, XPS or EXAFS of local coordination) will further refine these design principles. Altogether, this work transforms compositional complexity from a challenge into a tunable variable, offering quantitative, atomic-level rules for optimizing HE-MXenes in hydrogen evolution and related electrochemical reactions.

Conclusions

In summary, we have conducted a comprehensive high-throughput DFT study to investigate the HER activity of HE-MXenes, focusing on the influence of local atomic environments around surface oxygen terminations. By generating randomized atomic configurations on TiVNbMo-based HE-MXenes, we reveal that the identity of the first-nearest neighbor metal atom plays a dominant role in governing hydrogen adsorption strength. A consistent activity trend, V < Mo < Ti < Nb, was observed, with Ti- and Nb-rich local environments exhibiting the most favorable ΔG_H values for the HER. Notably, although Mo-based MXenes are commonly regarded as highly active HER catalysts in pristine or low-component systems, our results reveal that this trend does not universally extend to high-entropy MXenes. In these chemically complex systems, catalytic behavior is governed primarily by local coordination effects rather than by the presence of any single metal element. Through machine learning analysis, we identify the average covalent radius of S1 atoms as a physically meaningful and predictive descriptor for hydrogen adsorption free energy. This enables rapid and efficient screening of HER-active configurations without the need for exhaustive DFT calculations. Our findings highlight the importance of local atomic configurations in modulating catalytic performance and establish a structure–property relationship that can guide the rational design of HE-MXene-based electrocatalysts. This approach may be generalized to other catalytic reactions and compositional spaces, paving the way for data-driven discovery of next-generation high-entropy materials for sustainable energy applications.

Author contributions

Hao Yuan: conceptualization, methodology, formal analysis, investigation, writing – original draft, review, and editing. Jing Yang: formal analysis, methodology, and writing – review and editing. Yong-Wei Zhang: conceptualization, funding acquisition, supervision, project administration, and writing – review and editing.

Conflicts of interest

There are no conflicts to declare.

Data availability

All data needed to support the conclusions in the paper are presented in the paper and the supplementary information (SI). Supplementary information is available. See DOI: https://doi.org/10.1039/d6nr00514d.

The data are available at https://github.com/Yuanhaoooo/HEMXenes.

Acknowledgements

This work was supported by the Italy-Singapore Science and Technology Cooperation Programme (R22I0IR121) and the A*STAR Computational Centre and National Supercomputer Centre, Singapore.

References

1 E. S. Hanley, J. Deane and B.Ó Gallachóir, The Role of Hydrogen in Low Carbon Energy Futures-A Review of Existing Perspectives, *Renewable Sustainable Energy Rev.*, 2018, **82**, 3027–3045.
2 I. Staffell, D. Scamman, A. V. Abad, P. Balcombe, P. E. Dodds, P. Ekins, N. Shah and K. R. Ward, The Role of Hydrogen and Fuel Cells in the Global Energy System, *Energy Environ. Sci.*, 2019, **12**, 463–491.
3 S. Dunn, Hydrogen Futures: Toward A Sustainable Energy System, *Int. J. Hydrogen Energy*, 2002, **27**, 235–264.
4 J. A. Turner, A Realizable Renewable Energy Future, *Science*, 1999, **285**, 687–689.
5 D. Pashchenko, First Law Energy Analysis of Thermochemical Waste-heat Recuperation by Steam Methane Reforming, *Energy*, 2018, **143**, 478–487.
6 M. Ball and M. Wietschel, The Future of Hydrogen-Opportunities and Challenges, *Int. J. Hydrogen Energy*, 2009, **34**, 615–627.
7 S. E. Hosseini and M. A. Wahid, Hydrogen Production from Renewable and Sustainable Energy Resources: Promising Green Energy Carrier for Clean Development, *Renewable Sustainable Energy Rev.*, 2016, **57**, 850–866.
8 A. C. Chang, H.-F. Chang, F.-J. Lin, K.-H. Lin and C.-H. Chen, Biomass Gasification for Hydrogen Production, *Int. J. Hydrogen Energy*, 2011, **36**, 14252–14260.
9 I. Dincer and C. Acar, Review and Evaluation of Hydrogen Production Methods for Better Sustainability, *Int. J. Hydrogen Energy*, 2015, **40**, 11094–11111.
10 Z. W. Seh, J. Kibsgaard, C. F. Dickens, I. Chorkendorff, J. K. Nørskov and T. F. Jaramillo, Combining Theory and Experiment in Electrocatalysis: Insights into Materials Design, *Science*, 2017, **355**, eaad4998.
11 Z. Y. Yu, Y. Duan, X. Y. Feng, X. Yu, M. R. Gao and S. H. Yu, Clean and Affordable Hydrogen Fuel from Alkaline Water Splitting: Past, Recent Progress, and Future Prospects, *Adv. Mater.*, 2021, **33**, 2007100.
12 X. Zou and Y. Zhang, Noble Metal-Free Hydrogen Evolution Catalysts for Water Splitting, *Chem. Soc. Rev.*, 2015, **44**, 5148–5180.
13 Z. W. Seh, K. D. Fredrickson, B. Anasori, J. Kibsgaard, A. L. Strickler, M. R. Lukatskaya, Y. Gogotsi, T. F. Jaramillo and A. Vojvodic, Two-dimensional Molybdenum Carbide (MXene) as An Efficient Electrocatalyst for Hydrogen Evolution, *ACS Energy Lett.*, 2016, **1**, 589–594.
14 J. Zhang, Y. Zhao, X. Guo, C. Chen, C.-L. Dong, R.-S. Liu, C.-P. Han, Y. Li, Y. Gogotsi and G. Wang, Single Platinum Atoms Immobilized on An MXene as An Efficient Catalyst for the Hydrogen Evolution Reaction, *Nat. Catal.*, 2018, **1**, 985–992.
15 K. R. G. Lim, M. Shekhirev, B. C. Wyatt, B. Anasori, Y. Gogotsi and Z. W. Seh, Fundamentals of MXene Synthesis, *Nat. Synth.*, 2022, **1**, 601–614.
16 X. Bai, C. Ling, L. Shi, Y. Ouyang, Q. Li and J. Wang, Insight into the Catalytic Activity of MXenes for Hydrogen Evolution Reaction, *Sci. Bull.*, 2018, **63**, 1397–1403.
17 X. Wang, C. Wang, S. Ci, Y. Ma, T. Liu, L. Gao, P. Qian, C. Ji and Y. Su, Accelerating 2D MXene Catalyst Discovery for the Hydrogen Evolution Reaction by Computer-Driven Workflow and An Ensemble Learning Strategy, *J. Mater. Chem. A*, 2020, **8**, 23488–23497.
18 D. Jin, L. R. Johnson, A. S. Raman, X. Ming, Y. Gao, F. Du, Y. Wei, G. Chen, A. Vojvodic and Y. Gogotsi, Computational Screening of 2D Ordered Double Transition-Metal Carbides (MXenes) as Electrocatalysts for Hydrogen Evolution Reaction, *J. Phys. Chem. C*, 2020, **124**, 10584–10592.
19 S. G. Peera, R. Koutavarapu, L. Chao, L. Singh, G. Murugadoss and G. Rajeshkhanna, 2D MXene Nanomaterials as Electrocatalysts for Hydrogen Evolution Reaction (HER): A Review, *Micromachines*, 2022, **13**, 1499.
20 S. K. Nemani, B. Zhang, B. C. Wyatt, Z. D. Hood, S. Manna, R. Khaledialidusti, W. Hong, M. G. Sternberg, S. K. Sankaranarayanan and B. Anasori, High-Entropy 2D Carbide MXenes: $TiVNbMoC_3$ and $TiVCrMoC_3$, *ACS Nano*, 2021, **15**, 12815–12825.
21 P. E. Blöchl, Projector Augmented-Wave Method, *Phys. Rev. B: Condens. Matter Mater. Phys.*, 1994, **50**, 17953.
22 G. Kresse and D. Joubert, From Ultrasoft Pseudopotentials to the Projector Augmented-Wave Method, *Phys. Rev. B: Condens. Matter Mater. Phys.*, 1999, **59**, 1758.
23 J. P. Perdew, K. Burke and M. Ernzerhof, Generalized Gradient Approximation Made Simple, *Phys. Rev. Lett.*, 1996, **77**, 3865.
24 G. Kresse and J. Furthmüller, Efficient Iterative Schemes for Ab Initio Total-Energy Calculations Using A Plane-Wave Basis Set, *Phys. Rev. B: Condens. Matter Mater. Phys.*, 1996, **54**, 11169.

25 G. Kresse and J. Furthmüller, Efficiency of *Ab initio* Total Energy Calculations for Metals and Semiconductors using A Plane-Wave Basis Set, *Comput. Mater. Sci.*, 1996, **6**, 15–50.
26 S. Grimme, J. Antony, S. Ehrlich and H. Krieg, A Consistent and Accurate Ab Initio Parametrization of Density Functional Dispersion Correction (DFT-D) for the 94 Elements H-Pu, *J. Chem. Phys.*, 2010, **132**, 154104.
27 J. K. Nørskov, J. Rossmeisl, A. Logadottir, L. Lindqvist, J. R. Kitchin, T. Bligaard and H. Jonsson, Origin of the Overpotential for Oxygen Reduction at a Fuel-Cell Cathode, *J. Phys. Chem. B*, 2004, **108**, 17886–17892.
28 D. Liu, X. Xu, Y. Du, X. Qin, Y. Zhang, C. Ma, S. Wen, W. Ren, E. M. Goldys and J. A. Piper, Three-dimensional Controlled Growth of Monodisperse Sub-50 nm Heterogeneous Nanocrystals, *Nat. Commun.*, 2016, **7**, 10254.
29 Y. Jiang, T. Sun, X. Xie, W. Jiang, J. Li, B. Tian and C. Su, Oxygen–Functionalized Ultrathin $Ti_3C_2T_x$ MXene for Enhanced Electrocatalytic Hydrogen Evolution, *ChemSusChem*, 2019, **12**, 1368–1373.
30 F. Pedregosa, G. Varoquaux, A. Gramfort, V. Michel, B. Thirion, B. O. Grisel, M. Blondel, P. Prettenhofer, R. Weiss and V. Dubourg, Scikit-learn: Machine Learning in Python, *J. Mach. Learn. Res.*, 2011, **12**, 2825–2830.
31 A. Husile, Z. Wang and J. Guan, Applications of High-Entropy MOFs and Their Derivatives, *Coord. Chem. Rev.*, 2025, **533**, 216546.
32 L. Qi and J. Guan, Electronic Structure Modulation of High Entropy Materials for Advanced Electrocatalysis, *Green Energy Environ.*, 2025, **10**, 917–936.
33 Z. Zeng, X. Chen, K. Weng, Y. Wu, P. Zhang, J. Jiang and N. Li, Computational Screening Study of Double Transition Metal Carbonitrides M′2M′CNO_2-MXene as Catalysts for Hydrogen Evolution Reaction, *npj Comput. Mater.*, 2021, **7**, 80.
34 H. W. Seong, M. S. Lee and H. J. Ryu, First-principles Study for Discovery of Novel Synthesizable 2D High-entropy Transition Metal Carbides (MXenes), *J. Mater. Chem. A*, 2023, **11**, 5681–5695.
35 L. Xiao, Z. Wang and J. Guan, Optimization Strategies of High-Entropy Alloys for Electrocatalytic Applications, *Chem. Sci.*, 2023, **14**, 12850–12868.
36 L. H. Mou, T. Han, P. E. Smith, E. Sharman and J. Jiang, Machine learning descriptors for data-driven catalysis study, *Adv. Sci.*, 2023, **10**, 2301020.
37 A. Usuga, C. Praveen and A. Comas-Vives, Local descriptors-based machine learning model refined by cluster analysis for accurately predicting adsorption energies on bimetallic alloys, *J. Mater. Chem. A*, 2024, **12**, 2708–2721.
38 W. Xu, E. Diesen, T. He, K. Reuter and J. T. Margraf, Discovering high entropy alloy electrocatalysts in vast composition spaces with multiobjective optimization, *J. Am. Chem. Soc.*, 2024, **146**, 7698–7707.
39 X. Bai and J. Guan, Applications of MXene-based single-atom catalysts, *Small Struct.*, 2023, **4**, 2200354.